Calculation of frequency-dependent polarizabilities with application to photodetachment threshold shift in a strong laser field

M. Kutzner, H. P. Kelly, D. J. Larson, and Z. Altun*

Jesse W. Beams Laboratory of Physics, Department of Physics, University of Virginia, Charlottesville, Virginia 22901

(Received 7 June 1988)

Calculations of the frequency-dependent electric dipole polarizabilities have been carried out for atomic Cl and Cl$^-$ using many-body perturbation theory. Higher-order diagrams have been evaluated to include the effects of electron correlation. These results are used to interpret a recent experimental observation of shifts in the photodetachment threshold of Cl$^-$ in the presence of a strong laser field.

I. INTRODUCTION

The frequency-dependent electric dipole polarizability is an important parameter in the description of atomic processes including the ac Stark shift,[1] photoionization,[2] and the London dispersion forces between two atoms.[3] Very accurate calculations and precise measurements for the static polarizability and hyperpolarizability are now available for many atomic systems. These are discussed in the excellent review article by Miller and Bederson.[4] Dynamic polarizabilities, however, have been published for only a few neutral atoms[5-7] and negative ions.[8-10]

A recent experiment by Trainham et al.[11] measured approximately a 2-cm^{-1} increase in the Cl$^-$ photodetachment threshold in the presence of a 1064-nm wavelength, 10^{10} W/cm^2 laser field. Dynamic threshold shifts for negative ions have been anticipated theoretically by a number of authors[12] and shifts in photoionization thresholds have been extensively discussed in relation to the electron energy distribution observed in above-threshold ionization (ATI) experiments in neutral atoms.[13-15] However, the experiment of Trainham et al. provides the first *direct* observation of such a shift. This shift in the threshold is presumably due to a combination of dynamic Stark shifts for the negative ion and neutral atom, and the ponderomotive energy of free electron.[14,16] Calculation of the shift requires a knowledge of the ac Stark shifts for both the Cl$^-$ ion and the neutral atom Cl. Evaluation of these shifts and comparison to the ponderomotive energy provides a quantitative prediction for the Cl$^-$ threshold shift and a qualitative picture of what can be expected for similar measurements in other atomic systems.

The present paper presents many-body perturbation theory (MBPT) calculations of the dynamic polarizabilities of Cl$^-$ and neutral Cl. Section II contains a brief review of the theory. In Sec. III details of the calculations are given and the results are presented. Applications of the polarizability results to the experiment of Trainham et al.[11] and the implications for other experiments are discussed in the final section.

II. THEORY

The dynamic polarizability $\alpha(\omega)$ describes the linear response of an atom to an externally applied electric field and is defined by the equation

$$\mathbf{p} = \alpha(\omega)\mathbf{E} , \tag{1}$$

where $\mathbf{p}$ is the electric dipole moment and $\mathbf{E}$ is the applied field given by

$$\mathbf{E} = F\mathbf{z}\cos(\omega t) = F\mathbf{z}(e^{i\omega t} + e^{-i\omega t})/2 . \tag{2}$$

An atom in this field may be described in the nonrelativistic approximation by the Hamiltonian

$$H = \sum_{i=1}^{N} -\left[\frac{\nabla_i^2}{2}\right] - \frac{Z}{r_i} + \sum_{i<j=1}^{N} v_{ij} + F\cos(\omega t)\sum_{i=1}^{N} z_i , \tag{3}$$

where the first term represents the kinetic energy of each of the N electrons, the second term represents the interaction of each electron with the nucleus, the third term represents the Coulomb interaction between electron pairs, and the last term represents the interaction between each electron and the perturbing electric field $F\mathbf{z}\cos(\omega t)$. This Hamiltonian is manifestly gauge invariant since we have represented the interaction between electrons and the field in terms of $\mathbf{E}\cdot\mathbf{r}$ as opposed to the minimal substitution procedure.[17] Atomic units are employed throughout this paper unless otherwise indicated.

The dynamic polarizability of the atom is[2]

$$\alpha(\omega) = -\sum_{f(\neq n)} \left|\left\langle \psi_f \left| \sum_{i=1}^{N} z_i \right| \psi_n \right\rangle\right|^2 \times \left[\frac{1}{E_n - E_f - \omega} + \frac{1}{E_n - E_f + \omega}\right] , \tag{4}$$

where $\sum_{f(\neq n)}$ represents both a sum over bound excited states and an integral over continuum states. In Eq. (4) the wave functions ψ_n and ψ_f are exact eigenstates of the

nonrelativistic Hamiltonian with $F=0$. When ω is greater than the ionization threshold, the second denominator of Eq. (4) may vanish. In this case the denominator is treated in the usual way,[18,19] by adding a small imaginary contribution $i\eta$ to the denominator and taking the limit as $\eta \to 0$. We then have

$$\lim_{\eta \to 0^+} (E_n - E_f + \omega + i\eta)^{-1} = P(E_n - E_f + \omega)^{-1}$$
$$- i\pi\delta(E_n - E_f + \omega) , \qquad (5)$$

where P indicates a principal-value integration. The imaginary part of $\alpha(\omega)$ obtained from this expression leads to photodetachment or photoionization and is related to the cross section by the equation[2]

$$\sigma(\omega) = \frac{4\pi}{c} \omega \, \mathrm{Im}\alpha(\omega) . \qquad (6)$$

The real and imaginary parts of $\alpha(\omega)$ are related through the Kramers-Kronig relation[20]

$$\mathrm{Re}\alpha(\omega) = \frac{2}{\pi} P \int_0^\infty \frac{\omega' \mathrm{Im}\alpha(\omega')}{\omega'^2 - \omega^2} d\omega' . \qquad (7)$$

For a complex atom, it is generally impossible to evaluate the many-body wave functions ψ_n and ψ_f exactly. Here, we employ the many-body perturbation theory of Brueckner[21] and Goldstone[22] as applied to atoms.[23] The Hamiltonian of Eq. (3) is divided into a time-independent and a time-independent part. By applying time-dependent perturbation theory,[2] we obtain Eq. (4). The time-independent part of the Hamiltonian is then further separated into a part H_0 consisting of only one electron operators and a correlation term H_c treated as a perturbation. Then

$$H = H_0 + H_c + F\cos(\omega t) \sum_{i=1}^N z_i , \qquad (8)$$

where

$$H_0 = \sum_{i=1}^N \left[-\frac{\nabla_i^2}{2} - \frac{Z}{r_i} + V(r_i) \right] \qquad (9)$$

and

$$H_c = \sum_{i<j=1}^N v_{ij} - \sum_{i=1}^N V(r_i) . \qquad (10)$$

There is freedom in the choice of the single-particle potential $V(r_i)$, and important correlations may be included by selecting the potential judiciously. Experience has led us to choose either a term-dependent Hartree-Fock potential, or in the case of many open-shell systems, the effective potential of Qian et al.[24]

In the Brueckner-Goldstone expansion,[23] the correlated wave function ψ_n (or ψ_f) is given by the sum of all linked diagrams starting from an unperturbed state Φ_n (or Φ_f), with the perturbation H_c, but with no interactions with the time-dependent perturbation $(F/2)e^{\pm i\omega t}\sum_i z_i$. Here the Φ_n (and Φ_f) are eigenfunctions of the unperturbed Hamiltonian of Eq. (9). In the static case, one may start from the perturbation $\sum_i z_i$ and derive a diagrammatic expansion[23] for $\alpha(\omega)$ involving

two interactions with the dipole perturbation $\sum_i z_i$ and any number of interactions with H_c. For the time-dependent case a similar diagrammatic expansion[23] may be developed for $\alpha(\omega)$ where energy denominators between the two dipole interactions have additional terms $\pm\omega$. When electron correlations are neglected, we get the result of Eq. (4) where ψ_f and ψ_n are unperturbed states. The lowest-order diagrams contributing to $\alpha(\omega)$ are given in Fig. 1. In these diagrams, time proceeds from bottom to top. Particles are represented by arrows pointing upward. Hole states are represented by arrows pointing downward. The dashed line terminated by a dot represents an interaction with the electromagnetic field. If the bottom interaction is with $e^{+i\omega t}\sum_i z_i$, then the top interaction is with $e^{-i\omega t}\sum_i z_i$ and vice versa. Energy denominators at times preceding or following both interactions with the field are $E_0 - H_0$, while energy denominators occurring between the two interactions are $E_0 - H_0 \pm \omega$ when the initial interaction is with $e^{\pm i\omega t}\sum_i z_i$. Dashed lines indicate interactions through the perturbation H_c. Exchange diagrams are also included but are not pictured in Fig. 1. The lowest-order diagram is pictured in Fig. 1(a). This diagram is evaluated by substituting the eigenfunctions of H_0 into Eq. (4). When the interaction between electron pairs occurs before or after all interactions with the photon field, as in Figs. 1(b)–1(d), the diagram is an initial-state correlation diagram. When correlations occur between interactions with the photon field as in Fig. 1(e), the diagram is an intermediate-state correlation diagram.

The dipole matrix elements of Eq. (4) may be evaluated using two different operators: the length operator $Z = \sum_{i=1}^N z_i$, or the velocity operator $P_z = \sum_{i=1}^N p_{z_i}$. The two forms of the matrix element are related through the commutation relation

$$P_z = \frac{1}{i}[Z, H] , \qquad (11)$$
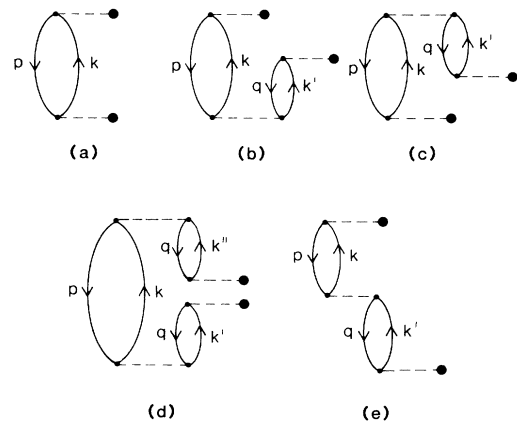

(a)   (b)   (c)

(d)   (e)

FIG. 1. Diagrams contributing to $\alpha(\omega)$: The heavy dot indicates an interaction with the external field. The bottom interaction is with $(F/2)e^{\pm i\omega t}\sum_i z_i$, and the top interaction is with $(F/2)e^{+i\omega t}\sum_i z_i$. (a) is the lowest-order diagram. (b), (c), and (d) are initial-state correlation diagrams. (e) is an intermediate-state correlation diagram.

which gives

$$\langle \psi_n \mid P_z \mid \psi_f \rangle = -i \langle \psi_n \mid ZH - HZ \mid \psi_f \rangle$$

$$= i(E_n - E_f)\langle \psi_n \mid Z \mid \psi_f \rangle . \qquad (12)$$

Recall that ψ_n and ψ_f are eigenstates of H in the absence of the time-dependent electric field. We have evaluated the dynamic polarizability using both length and velocity forms of the dipole operator; the two results must agree when electron correlations have been included to all orders. The calculations were performed with $\mathbf{E} \cdot \mathbf{r}$ as the time-dependent perturbation added to the time-independent Hamiltonian $H_0 + H_c$ of Eqs. (9) and (10). Velocity results were obtained by substitution of $\langle \psi_n \mid P_z \mid \psi_f \rangle / i(E_n - E_f)$ for $\langle \psi_n \mid Z \mid \psi_f \rangle$ in Eq. (4). The choice of gauge and its effect on the interpretation of threshold shifts is discussed in Sec. IV.

III. CALCULATIONS AND RESULTS
A. The negative chloride ion, Cl⁻

Calculation of the Cl⁻ polarizability is simplified by two considerations: the closed shell properties which limit the number of LS-coupled states to be considered and the absence of any bound excited states. We calculated both the real and imaginary parts of $\alpha(\omega)$. Calculations of the photoionization cross section for Cl⁻ have already been performed including interesting higher-order effects such as the polarization potential and relaxation.[25] Relativistic random-phase-approximation calculations have also been reported.[26] Thus, the imaginary part of $\alpha(\omega)$ [which is proportional to the photoionization cross section through Eq. (6)] is of interest as it is related to the real part [through Eq. (7)], and since it can be compared to other calculations, it is a check on our method.

Orbitals representing the ground state were generated by the multiconfiguration Hartree-Fock (MCHF) code of Fischer.[27] A set of 46 continuum s orbitals and 46 continuum d orbitals used in the integrals over excited states were calculated in the $3p^5(^2P)ks(^1P)$ and $3p^5(^2P)kd(^1P)$ $V^{(N-1)}$ potentials, respectively. A projection operator method was used to ensure orthogonality between the excited s orbitals and the ground state s orbitals.[28] Throughout the calculation we used the single particle $3p$ hole energy of -0.1503 a.u. obtained from the single-configuration ground-state MCHF calculation. The experimental photodetachment threshold is 0.134 a.u. (Ref. 29) and the difference in the total self-consistent-field energies of the neutral atom and the ion (ΔSCF energy) is 0.0948 a.u.

The lowest-order diagram contributing to the polarizability is shown in Fig. 1(a) and is given by

$$\alpha(\omega) = -\sum_k \mid \langle k \mid z \mid p \rangle \mid^2 \left[\frac{1}{\epsilon_p - \epsilon_k + \omega} + \frac{1}{\epsilon_p - \epsilon_k - \omega} \right],$$

$$(13)$$

where $\sum_k$ represents the sum over bound excited states (if any) and integral over continuum states, and ϵ is the single-particle energy. In Cl⁻ we calculated this diagram
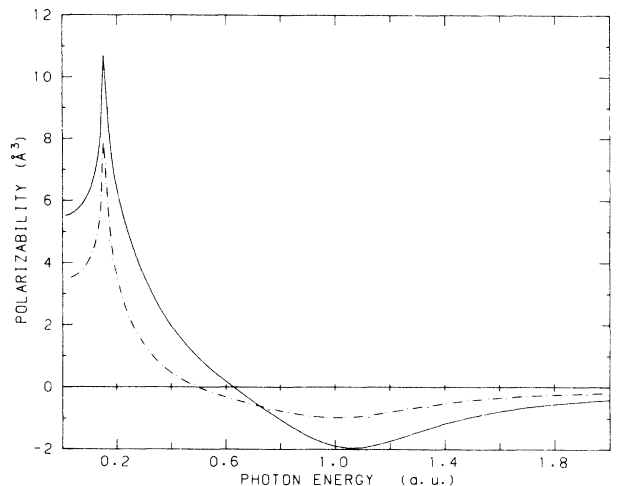

FIG. 2. Real part of $\alpha(\omega)$ for Cl⁻ plotted as a function of photon energy (frequency in a.u.). Only the lowest-order diagrams were included in this calculation. Length result indicated by ——, velocity by —·—·—·.

for $p = 3p$, $k = ks$, kd; $p = 3s$, $k = kp$; and $p = 2p$, $k = ks, kd$. The effects of the $3s$ and $2p$ excitations were found to be quite small because the binding energies are relatively large (0.73 and 7.70 a.u., respectively, in the Hartree-Fock approximation). The results of this zeroth-order calculation are plotted in Fig. 2. Although the length and velocity calculations show similar trends as a function of the frequency of the applied field, they disagree quantitatively.

The differences between the individual length and velocity calculations indicate the need for the inclusion of correlations. The higher-order diagrams of Figs. 1(b)–1(e) were evaluated and added to the lowest-order result. The initial-state correlation diagrams of Figs. 1(b)–1(d) were evaluated for $p = 3p$, $k = kd, ks$; $p = 3s$, $k = kp$; with $q = 3p$, $k' = kd, ks$; $q = 3s$, $k' = kp$; $q = 2p$, $k' = ks, kd$. The intermediate-state correlation diagrams of Fig. 1(e) were evaluated for $p = q = 3p$ and either $k = ks$, $k' = kd$ or $k = kd$, $k' = ks$. The case where k and k' have the same orbital angular momentum is accounted for by our use of the LS-coupled potential. The results obtained by summing these diagrams are displayed in Fig. 3. Here the length and velocity results are in far better agreement with one another than in Fig. 2.

Our value for the static polarizability, $\alpha(\omega = 0)$, is 4.37 Å³ (length) and 4.29 Å³ (velocity). This is to be compared with the coupled Hartree-Fock result by McEachran et al.[30] of 4.675 Å³ and the early estimate by Dalgarno[31] of $\simeq 3$ Å³. The polarizability for Cl⁻ was first measured by Fajans and Bauer[32] in an aqueous electrolyte solution and later corrected by Coker[33] for the perturbing effects of the aqueous solvent to a value of 4.11(6) Å³. Our result differs from this value by 5%. For static polarizabilities, we do not claim the high degree of accuracy obtained by Werner and Meyer[34] and Reinsch and Meyer[35] using pseudonatural orbital configuration interaction. Their calculation produces polarizabilities
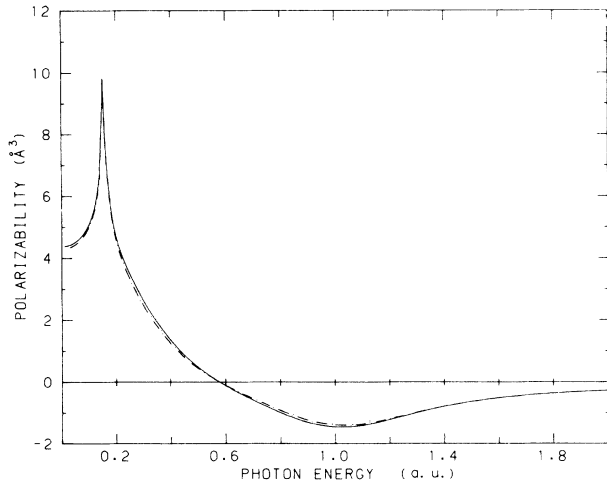
FIG. 3. Real part of $\alpha(\omega)$ for Cl$^-$ including higher-order MBPT diagrams shown in Figs. 1(b)–1(e); ——, length result; —·—·—·, velocity result.

FIG. 5. Imaginary part of $\alpha(\omega)$ for Cl$^-$ including higher-order MBPT diagrams shown in Figs. 1(b)–1(e); ——, length result; ··········, velocity result.

which they state are accurate to 2% for many neutral atoms. We have left out many higher-order diagrams which could conceivably alter our value for the static polarizability by as much as 10%. Examples of such diagrams are shown in Fig. 4. However, we believe that our level of accuracy is appropriate for purposes of comparison to threshold shift measurements in laser fields.

An essential element of the present calculation is the determination of the frequency-dependence of the polarizability. The increase in polarizability as ω increases from zero can be seen by expanding the denominators in Eq. (13) in powers of ω. The peak occurring at the photodetachment threshold results from the cancellation between ϵ_p and ω in the denominator of this term. This is consistent with the below threshold behavior of the analytic expression for $\alpha(\omega)$ derived by Aldelman[8] for H$^-$ and with the quasiclassical description for negative alkali-metal ions given by Delone et al.[9] The analytic expressions derived by Dalidchik and Slonim[10] for negative ions with a valence p electron do not have the correct behavior for $\alpha(\omega)$ as $\omega \rightarrow 0$.

Our calculations of $\alpha(\omega)$ increase to a finite peak at the photodetachment threshold (we have used the Hartree-Fock eigenvalue energy of 0.1503 a.u.). A finite max-
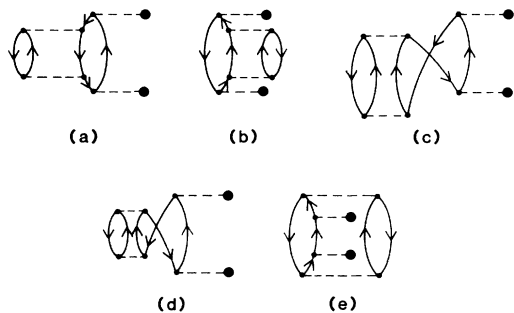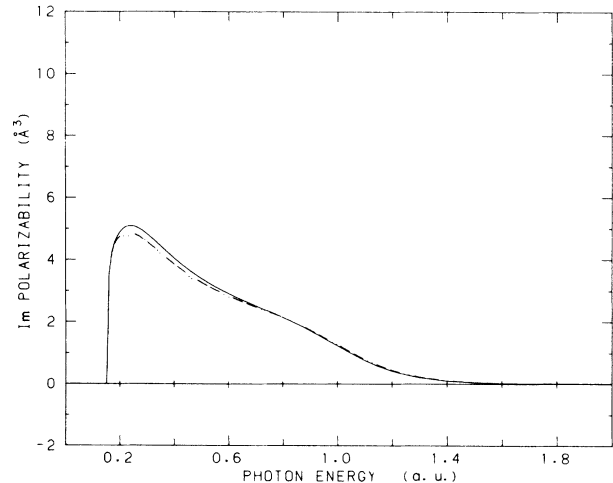
imum for this peak is expected for the following reason. The excited-state single-particle orbitals, P_{kl} for Cl$^-$ (or any negative ion) are calculated in a potential where Coulomb forces are neutralized by screening and can be approximated by spherical Bessel functions $j_l(kr)$. In the k-normalization scheme in which

$$P_{kl}(r) \sim \sin(kr - l\pi/2 + \delta_l) , \qquad (14)$$

the spherical Bessel functions are multiplied by kr. For small kr, these functions are proportional to $(kr)^{l+1}$, hence the dipole matrix elements scale as k for s waves and k^3 for d waves. The integrand in Eq. (13) thus remains finite as k approaches zero, even when ϵ_p and ω cancel.

When the frequency of the applied field greatly exceeds the orbital frequency of the $3p$ electrons, we see a negative result consistent with the $-1/\omega^2$ result expected for free electrons. This point is discussed further in Sec. IV.

As a check on our calculation of the real part of $\alpha(\omega)$, we used the result for the imaginary part obtained using the second term in Eq. (5) and shown in Fig. 5 as input to the right-hand side of Eq. (7). The real part of $\alpha(\omega)$ obtained in this way agrees with the independent calculation of Re$[\alpha(\omega)]$ to within 5% at most frequencies.

B. Neutral chlorine

The neutral chlorine calculation is complicated by the presence of bound excited states in addition to the continuum, as well as nine different multiplet terms which are accessible from the ground state through the dipole operator. This is to be compared with Cl$^-$ which has only two continuum channels corresonding to $3p^5kd(^1P)$ and $3p^5ks(^1P)$ originating from the $3p$ valence shell. We have used the Russell-Saunders LSM_LM_S coupling scheme throughout this calculation. A detailed MBPT calculation of the photoionization cross section for neutral chlorine which includes couplings between the many final-state channels has been performed by Brown et al.[36]

(a)   (b)   (c)

(d)   (e)

FIG. 4. Higher-order diagrams contributing to $\alpha(\omega)$. These are not included in the present calculation.

It was shown, however, by Qian et al.[24] that by a suitable choice of an effective potential, many of the effects of the final-state correlations may be included. We have chosen to simplify the present calculation by using this latter potential.

Neutral chlorine has the open-shell ground-state configuration $3p^5(^2P)$. The terms which are accessible from the ground state by excitation of a $3p$ electron by the dipole operator are $3p^4(^1D)kd(^2D)$, $3p^4(^3P)kd(^2D)$, $3p^4(^1S)kd(^2D)$, $3p^4(^1D)kd(^2P)$, $3p^4(^3P)kd(^2P)$, $3p^4(^1D)kd(^2S)$, $3p^4(^1D)ks(^2D)$, $3p^4(^3P)ks(^2P)$, and $3p^4(^1S)ks(^2S)$. Rather than calculate six different sets of d orbitals and three different sets of s orbitals, we calculated a single set of d and s orbitals in the appropriate potentials.[24]

Having obtained a complete set of excited states in this fashion, we summed the MBPT diagrams of Fig. 1. The virtual excited states are LS-coupled wave functions so that, in general, a different diagrammatic series must be summed for each LS-coupled intermediate state. For $3p \rightarrow kd$ excitations, six sets of LS-coupled states are used to evaluate the diagrams of Fig. 1, and for $3p \rightarrow ks$ there are three sets of LS-coupled states. In addition the polarizability was averaged over M_L.

It is desirable to include the effects of the various photoionization edges due to the ^3P, ^1D, and ^1S couplings. The experimental $3p$ removal energies 0.4800 (^3P), 0.5315 (^1D), and 0.6055 (^1S) a.u. for each of these ionic core couplings were used in calculating the diagrams.[37]

Brown et al.[36] noted in the photoionization calculation that exciting a $3s$ electron into the open $3p$ shell has a large effect because of the near degeneracy between the $3s$ and $3p$ shells. This excitation was treated by calculating the $3s3p^6(^2S)$ state self-consistently, and using the resulting $3p$ orbital to evaluate the diagram of Fig. 1(a) with $p = 3s$ and $k = 3p$. The excitation energy of the $3s3p^6(^2S)$ state was taken to be 0.3904 a.u., the value measured by Radziemski and Kaufman.[38] No higher-order diagrams were included for the $3s3p^6(^2S)$ excitation.

The lowest-order result represented by the diagram of Fig. 1(a) where $p = 3p$, $k = ks$, kd and $p = 3s$, $k = 3p$ is shown in Fig. 6 for both length and velocity forms. Again the length and velocity agreement is only fair. Resonances corresponding to the excitations $3p \rightarrow nd$ and $3p \rightarrow ns$ converging to the ^3P, ^1D, and ^1S thresholds begin at 0.34 a.u. Only the first of these excitations are shown due to the complexity of the spectrum in this region. We have not included the higher-order diagrams which would contribute to resonance width, so the resonances appear as simple poles. The large peak seen at 0.39 a.u. is due to the $3s3p^6(^2S)$ excitation and is not a member of these Rydberg series; we get a contribution to $3s \rightarrow 3p$ only for $M_L = 0$.

The real part of the frequency-dependent polarizability for neutral chlorine calculated with all the diagrams of Fig. 1 is shown in Fig. 7. For Fig. 1(e) we only included coupling between $3p \rightarrow ks$ and $3p \rightarrow kd$ channels. These diagrams are not included by our choice of potential. The average potential includes the effects of the diagram of Fig. 1(e) when $p = q$ and k and k' have the same angular momentum. The agreement between length and ve-
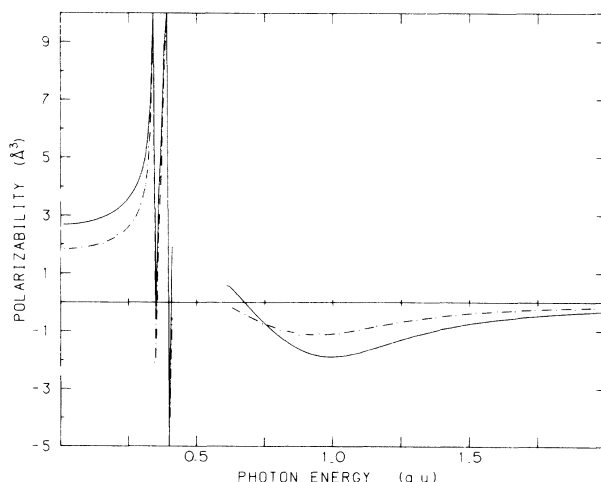

FIG. 6. Real part of $\alpha(\omega)$ for Cl including only the lowest-order MBPT diagrams. Length result indicated by ———, velocity by —·—·—·. Resonance widths were not calculated.

locity results is now very good. Our calculated static polarizability $\alpha(\omega=0)$ is 2.22 Å^3 (length) and 2.16 Å^3 (velocity). The geometric mean is 2.19 Å^3 and is in close agreement with the accurate calculations of Reinsch and Meyer[35] of 2.18(4) Å^3. We do not expect the accuracy of our calculation to be better than approximately 10% because of the neglect of additional diagrams. Thus, our very close agreement with Reinsch and Meyer may be fortuitous. When the $3s \rightarrow 3p$ excitation is not included, the static polarizability is 1.95 Å^3, so the contribution of the $3s3p^6(^2S)$ state is significant. We are unaware of any experimental measurements of the polarizability of neutral chlorine.

In Fig. 8 we give the corresponding calculated imaginary part of the polarizability. These results are in close agreement with the photoionization cross-section result of Qian et al.[24] without the factor $4\pi\omega/c$ of Eq. (6).
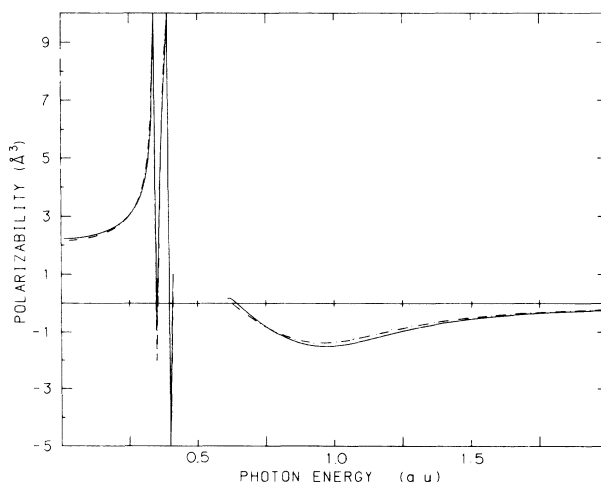

FIG. 7. Real part of $\alpha(\omega)$ for Cl including higher-order diagrams. ——— is the length result, —·—·—·. is the velocity result. Resonance widths have not been calculated.
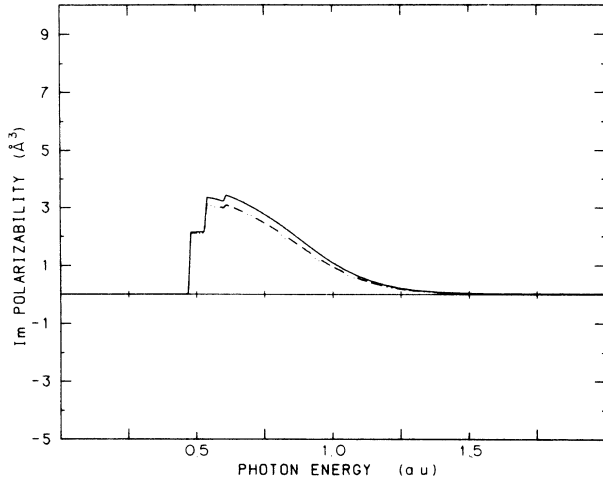
FIG. 8. Imaginary part of $\alpha(\omega)$ for Cl including higher-order diagrams. —— is the length result, --------- is the velocity result.

IV. DISCUSSION

A principal motivation for the present calculations was the recent report by Trainham et al.[11] of an increase in the photodetachment threshold of Cl^- in the presence of 1064-nm wavelength laser radiation. The experiment consisted of producing Cl^- ions in an ion trap and photodetaching the ions with ultraviolet light. This was done with and without the presence of the infrared laser light. With an infrared laser field intensity of 10^{10} W/cm² they were able to detect threshold shifts of approximately 2 cm^{-1}.

The contributions to the threshold shift can be identified using the energy conservation argument of Mittleman.[14] Applied to the problem of photodetachment such an argument gives[11]

$$E_{EA}(F) - E_{EA}(0) = U_p(\text{electron}) - U_p(\text{ion})$$

$$- \Delta W(\text{ion}) + \Delta W(\text{atom}) , \qquad (15)$$

where $E_{EA}(F)$ and $E_{EA}(0)$ are the electron affinities of the ion with and without the applied field, U_p (electron) is the ponderomotive energy[14,16] of a free electron $(e^2 F^2/4m\omega^2$, where F is the field amplitude), U_p(ion) is the ponderomotive energy of the ion, and ΔW(ion) and ΔW(atom) are the ac Stark shifts of the ion and the neutral atom.

There exist a number of discussions in the literature about the effects of different choices of gauge[39] on the calculation of transition probabilities and about the role of the ponderomotive potential[14,16] in threshold shifts.[13-15] The present calculations have been carried out using the manifestly gauge-invariant Hamiltonian which represents the interaction between particles and fields as $\mathbf{E} \cdot \mathbf{r}$. The agreement between our computed length and velocity results should therefore be regarded as an indication of how well the commutation relation of Eq. (12) holds, i.e., to what extent correlations have made ψ_n and ψ_f exact eigenstates of H with $F = 0$. Notice that our Hamiltonian

of Eq. (3) does not include terms involving motion of the center of mass. It is for this reason that the term U_p(ion) is included in the energy-balance equation [Eq. (15)].

The issue of choice of gauge can, at first, appear particularly troublesome for calculation of threshold shifts. Since the ponderomotive energy of the free electron is often viewed as arising from the A^2 term in the Coulomb gauge, and since this term contains no electron coordinates and therefore has the same value for the bound electron as the free electron, it may appear incorrect to find a threshold shift which depends upon the free-electron ponderomotive energy. Mittleman has stated that any interpretation of a shift in the ionization potential due to the A^2 term is erroneous.[40] This statement is literally correct. However, the ionization or photodetachment energy is dependent upon the strength of the applied field, and whether or not part of this dependence comes from the ponderomotive energy can be considered a matter of interpretation. In the case where the zero of energy is taken to be that of the free electron at rest outside the laser field, the threshold-energy shift is most naturally written in terms of the ponderomotive potential and Stark shifts as in Eq. (15).

The energy-level diagram of Fig. 9 serves to illustrate the shift in terms of the gauge which includes both a $\mathbf{p} \cdot \mathbf{A}$ and an $\mathbf{A}^2$ term. The left side illustrates the energy separation between the valence level G in the ground state of the ion and the zero kinetic energy threshold state T of the photoelectron when no laser field is present. The electron affinity $E_{EA}(0)$ when $F = 0$ is the difference between these two levels when relaxation effects are neglected. Introducing the laser field has different effects on the valence level G and the threshold state T. The valence level is reduced in energy by the $\mathbf{p} \cdot \mathbf{A}$ term in the Hamiltonian which is partly canceled, however, by the $\mathbf{A}^2$ term (the ponderomotive potential).[15] The remaining downward shift in level G is the shift obtained directly from $\mathbf{E} \cdot \mathbf{r}$ the quantity theoretically calculated in this paper. The threshold level T is shifted upward by the ponderomotive term alone since the average shift due to $\mathbf{p} \cdot \mathbf{A}$ on a
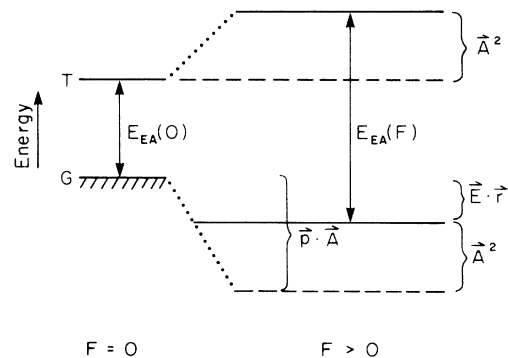

FIG. 9. Schematic of contributions to the threshold shift. G is the energy of the valence level of the ground state of the ion outside the applied field $(F = 0)$. T is the energy of the lowest-lying threshold level outside the field and is the zero energy for this analysis. $E_{EA}(F)$ and $E_{EA}(0)$ are the electron affinities with and without the field present. Qualitative contributions of the various terms of the Hamiltonian are shown as level shifts.

continuum electron is zero, where **p** is the canonical momentum.[41] The zero energy on this diagram is best referenced to level T with $F = 0$. Switching on the laser field thus has two discernable effects: (a) the photodetachment threshold is shifted by an amount $E_{EA}(F) - E_{EA}(0)$ given in Eq. (15) and (b) the photoelectrons leave the laser field with kinetic energy greater than or equal to the pondermotive energy. The second statement is true only in the case of continuous-wave or long-pulse laser fields, since the pondermotive force becomes nonconservative in a time-dependent field.[42-44]

In evaluating the shift predicted by Eq. (15), we observe that $U_p(\text{ion})$ is negligible since the mass of the ion is about 37 000 times that of the free electron. The ponderomotive energy of the free electron is 8.55 cm^{-1} at 10^{10} W/cm^2 for 1064 nm (1.16 eV) light. The ac Stark shifts for the ion and the atom may be obtained from the respective polarizabilities through the expression

$$\Delta W(\omega) = -(1/4)\alpha(\omega)F^2 , \tag{16}$$

where the field amplitude F defined in Eq. (2) is related to the laser intensity through the time-averaged Poynting vector

$$|\mathbf{S}| = (c/8\pi)|\mathbf{E} \times \mathbf{B}| = (c/8\pi)F^2 . \tag{17}$$

At 1064 nm the polarizabilities are seen from Fig. 3 and Fig. 7 to be 4.42 Å^3 for Cl$^-$ and 2.33 Å^3 for the neutral atom (geometric means of length and velocity). Hence, the difference between the ionic and atomic ac Stark shifts at 1064 nm and 10^{10} W/cm^2 is 0.24 cm^{-1}. This contribution to the threshold shift of Eq. (16) is small compared to the 8.55 cm^{-1} expected from the ponderomotive energy of the electron. The total predicted shift is 8.79 cm^{-1} at 10^{10} W/cm^2. Our analysis provides no explanation for the observation of a shift of approximately 2 cm^{-1}. The explanation may lie in some aspect of the experiment, such as the temporal variation of the laser light, not taken into account here.

While the ac Stark shift of the Cl$^-$ ground state is distinctly smaller in magnitude than the ponderomotive energy of the free electron at 1064 nm, the situation is reversed at higher frequencies. This can be easily seen in Fig. 10 where $\alpha_p = -e^2/m\omega^2$ is plotted along with $\alpha(\omega)$ for Cl$^-$ from Fig. 3. The quantity α_p is the polarizability equivalent of the free-electron ponderomotive energy; i.e., substituting α_p into Eq. (16) gives the ponderomotive energy. As the frequency is increased from zero, $\alpha(\omega)$ first exceeds α_p in magnitude just below the detachment
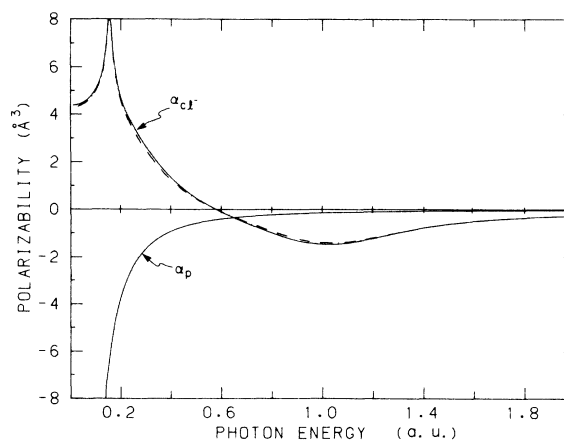

FIG. 10. Real $\alpha(\omega)$ for Cl$^-$ ——, length; —·—·—·, velocity; and $\alpha_p(\omega)$ the polarizability equivalent of the free electron ponderomotive energy $-e^2/m\omega^2$.

threshold at 0.1503 a.u. At a wavelength of 248 nm, where high-intensity laser-ionization experiments have been carried out,[44] $\alpha(\omega)$ is approximately 6 Å^3 and α_p is -4.4 Å^3. At frequencies above about 1.5 a.u., $\alpha(\omega)$ varies as $-1/\omega^2$ and the ratio of $\alpha(\omega)$ to α_p is approximately 6.9. This last observation can be understood from the following argument. At frequencies well above the orbital frequency of a valence electron in the ion, the electron jiggles in the laser field essentially as if it were free. Thus the electron will have an energy shift equal to the ponderomotive shift of a free electron. Since there are six equivalent valence electrons in Cl$^-$, we expect a shift of roughly six times the ponderomotive energy. This interpretation of the high-frequency limit of $\alpha(\omega)$ is in agreement with the result for negative alkali-metal ions obtained by a combination of a quasiclassical approach and the Hartree-Fock approximation,[9] where the behavior of $\alpha(\omega)$ averaged over the alkali-metal ions is $-2.157/\omega^2$ a.u. Clearly, the relative importance of the polarizability and the ponderomotive energy depends upon the frequency at which the experiment is done.

ACKNOWLEDGMENTS

*Present address: Marmara University, Fen-Ed. Fakültesi, Findikzade-Istanbul, Turkey.

[1]A. M. Bonch-Bruevich and V. A. Khodovoi, Usp. Fiz. Nauk. 93, 71 (1967) [Sov. Phys.—Usp 10, 637 (1968)].

[2]U. Fano and J. W. Cooper, Rev. Mod. Phys. 40, 441 (1968).

[3]C. Mavroyannis and J. M. Stephen, Mol. Phys. 5, 629 (1962).

[4]T. M. Miller and B. Bederson, Adv. At. Mol. Phys. 13, 1 (1977).

[5]H. P. Kelly, Phys. Rev. 182, 84 (1969).

[6]P. K. Mukherjee and R. K. Moitra, J. Phys. B 11, 2813 (1978); B. Kundu, D. Ray, and P. K. Mukherjee, Phys. Rev. A 34, 62 (1986).

[7]N. C. Dutta, T. Ishibara, C. Matsubara, R. T. Pu, and T. P. Das, Phys. Rev. Lett. 22, 8 (1969); P. E. S. Wormer and W. Rijks, Phys. Rev. A 33, 3138 (1986); E. A. Reinsch, J. Chem. Phys. 83, 5784 (1985); P. Shorer and K. T. Taylor, J. Phys. B 14, 4007 (1981).

[8]S. A. Adelman, Phys. Rev. A 5, 508 (1972).

[9]N. B. Delone, P. A. Golovinsky, I. Y. Keyan, V. P. Krainov, and A. I. Tuguchev, J. Phys. B 19, 2457 (1986).

[10]F. I. Dalidchik and V. Z. Slonim, Theor. Exp. Chem. 13, 1 (1977).

[11]R. Trainham, G. D. Fletcher, N. B. Mansour, and D. J. Larson, Phys. Rev. Lett. 59, 2291 (1987).

[12]K. Rzazewski, M. Lewenstein, and J. H. Eberly, J. Phys. B 15, L661 (1982); M. V. Federov and A. E. Kazakov, ibid. 16, 3641 (1983); M. V. Federov and A. E. Kazakov, ibid. 16, 3653 (1983); S. L. Haan and J. Cooper, ibid. 17, 3481 (1984); S. E. Kumekov and V. I. Perel, Zh. Eksp. Teor. Fiz. 81, 1693 (1981) [Sov. Phys.—JETP 54, 899 (1981)].

[13]P. Agostini, F. Fabre, G. Mainfray, G. Petite, and N. K. Rahman, Phys. Rev. Lett. 42, 1127 (1979); P. Kruit, J. Kimman, and M. J. van der Wiel, J. Phys. B 14, L597 (1981); L. A. Lompre, A. L'Huillier, G. Mainfray, and C. Manus, J. Opt. Soc. Am. B 2, 1906 (1985); A number of articles are collected in the feature on multielectron excitations in atoms, J. Opt. Soc. B 4, 705-862 (1987); H. G. Muller, A. Tip, and M. J. van der Wiel, J. Phys. B 16, L679 (1983).

[14]M. H. Mittleman, Phys. Rev. A 29, 2245 (1984).

[15]L. Pan, L. Armstrong, Jr., and J. H. Eberly, J. Opt. Soc. Am. B 3, 1319 (1986).

[16]M. H. Mittleman, J. Phys. B 17, L351 (1984); T. W. B. Kibble, Phys. Rev. 150, 1060 (1966); J. H. Eberly, Prog. Opt. 7, 359 (1969); P. Avan, C. Cohen-Tannoudji, J. Dupont-Roc, and C. Fabre, J. Phys. (Paris) 37, 993 (1976).

[17]M. Scadron, Advanced Quantum Theory and Its Application Through Feynman Diagrams (Springer-Verlag, New York, 1979), p. 52.

[18]B. Lippman and J. Schwinger, Phys. Rev. 79, 469 (1950).

[19]K. A. Brueckner, R. J. Eden, and N. C. Francis, Phys. Rev. 100, 891 (1955).

[20]J. D. Jackson, Classical Electrodynamics, 2nd ed. (Wiley, New York, 1975), p. 311.

[21]K. A. Brueckner, Phys. Rev. 97, 1353 (1955).

[22]J. Goldstone, Proc. R. Soc. London, Ser. A 239, 267 (1957).

[23]H. P. Kelly, Adv. Theor. Phys. 2, 75 (1968).

[24]Z. Qian, S. L. Carter, and H. P. Kelly, Phys. Rev. A 33, 1751 (1986).

[25]Z. Qian and H. P. Kelly (unpublished).

[26]V. Radojevic, H. P. Kelly, and W. R. Johnson, Phys. Rev. A 35, 2117 (1987).

[27]C. Froese-Fischer, Comput. Phys. Commun. 14, 145 (1978).

[28]L. M. Frantz, R. L. Mills, R. G. Newton, and A. M. Sessler, Phys. Rev. Lett. 1, 340 (1958); B. A. Lippmann, M. H. Mittleman, and K. M. Watson, Phys. Rev. 116, 920 (1959); R. T. Pu and E. S. Chang, ibid. 151, 31 (1966); H. J. Silverstone and M. L. Yin, J. Chem. Phys. 49, 2026 (1968); S. Huzinaga and C. Arnau, Phys. Rev. A 1, 1285 (1970).

[29]R. Trainham, G. D. Fletcher, and D. J. Larson, J. Phys. B 20, L777 (1987).

[30]R. P. McEachran, A. D. Stauffer, and S. Greita, J. Phys. B 12, 3119 (1979).

[31]A. Dalgarno, Adv. Phys. 11, 281 (1962).

[32]K. Fajans and N. Bauer, J. Am. Chem. Soc. 64, 3023 (1942).

[33]H. Coker, J. Phys. Chem. 80, 2084 (1976).

[34]H. J. Werner and W. Meyer, Phys. Rev. A 13, 13 (1976).

[35]E. A. Reinsch and W. Meyer, Phys. Rev. A 14, 915 (1976).

[36]E. R. Brown, S. L. Carter, and H. P. Kelly, Phys. Rev. A 21, 1237 (1980).

[37]C. E. Moore, Atomic Energy Levels, Natl. Bur. Stand. (U.S.) Circ. No. 467 (U.S. GPO, Washington, D.C., 1949), Vol. I.

[38]L. J. Radziemski, Jr. and V. Kaufman, J. Opt. Soc. Am. 59, 424 (1969).

[39]A. F. Starace, Phys. Rev. A 3, 1242 (1971); A. F. Starace, ibid. 8, 1141 (1973); I. P. Grant, J. Phys. B 7, 1458 (1974); I. P. Grant and A. F. Starace, ibid. 8, 1999 (1975).

[40]M. H. Mittleman, Introduction to the Theory of Laser-Atom Interactions (Plenum, New York, 1982), p. 37.

[41]R. Shakeshaft, Z. Phys. D 8, 47 (1988).

[42]L. Jönsson, J. Opt. Soc. Am. B 4, 1422 (1987).

[43]P. H. Bucksbaum, M. Bashkansky, and T. J. McIlrath, Phys. Rev. Lett. 58, 349 (1987).

[44]T. S. Luk, T. Graber, H. Jara, U. Johann, K. Boyer, and C. K. Rhodes, J. Opt. Soc. Am. B 4, 847 (1987).